RESEARCH ARTICLE

Pd-Ni nanoparticles supported on titanium oxide as effective catalysts for Suzuki-Miyaura coupling reactions

Dongxu Han, Zhiguo Zhang (✉), Zongbi Bao, Huabin Xing, Qilong Ren (✉)

Key Laboratory of Biomass Chemical Engineering of Ministry of Education, College of Chemical and Biological Engineering, Zhejiang University, Hangzhou 310027, China

Abstract We have successfully prepared a series of Pd-Ni/TiO$_2$ catalysts by a one-step impregnation-reduction method. Among these catalysts with different compositions of Ni and Pd, the one with the Ni:Pd ratio of 2.95 showed the best activity. Small monodispersed Pd-Ni bimetallic nanoparticles were loaded on the surface of titanium oxide nanopowder as confirmed with TEM and EDS mapping. The XPS analysis demonstrated that Pd exists as 31% Pd(II) species and 69% Pd(0) species and all nickel is Ni(II). The prepared Pd-Ni/TiO$_2$ exhibited enhanced catalytic activity compared to an equal amount of Pd/TiO$_2$ for Suzuki-Miyaura reactions together with excellent applicability and reusability.

Keywords Pd-Ni bimetallic nanoparticles, nanocatalysis, Suzuki-Miyaura reaction, titanium oxide

1 Introduction

Palladium-catalyzed Suzuki-Miyaura coupling reaction (SMR) is one of the most important approaches to form C–C bond. It has been widely applied to the synthesis of pharmaceutical intermediates, natural products, functional materials and biomolecules, due to its advantages such as mild reaction conditions and low toxicity [1–7]. Besides using organic ligands to finely tune catalytic activities of homogeneous Pd catalysts, reducing Pd particle size to nanoscale has also become a prevalent strategy to produce robust catalysts for the SMRs by increasing of atom efficiency, as other organic chemical reactions catalyzed by nanomaterials [3,8–10]. As a consequence, the SMRs catalyzed with Pd nanoparticles have received increasing attention in recent years. In comparison to homogeneous Pd catalysts, Pd nanoparticles can be readily separated from products and reused in succession without considerable loss of catalytic activity [11–17]. Nevertheless, from a practical point of view, it is still imperative to reduce the dosage of Pd catalyst for the SMR because of the limited reserves of noble metals.

In this respect, the development of bimetallic nanoparticles, in particular palladium with non-noble metals, has many advances over the past few years [18,19]. Bimetallic nanocatalysts not only combine the properties of individual constituents but also may have enhanced catalytic activity, selectivity, and stability. This may be attributed to the modulation of the charge transfer between different metals and surface element distribution [20,21]. In this context, Pd-based bimetallic nanoparticles (NPs) have been widely used in various coupling reactions, such as polypropylenimine-grafted graphene supported Pd-Co alloy NPs for the Sonogashira reaction and a PVP-stabilized Au-Pd alloy for the Ullmann reaction [22,23]. Chen and coworkers demonstrated that Au-Pd@SiO$_2$ with a core-shell structure of Au-Pd particles is better than monometallic palladium nanoparticles as a catalyst for the SMRs [24]. Muraviev and coworkers reported that a core-shell Pd@Co NPs based on cross-linked polymers showed enhanced catalytic activity and stability [25]. Recently, we have shown that TiO$_2$-supported bimetallic Au-Pd nanoparticles are efficient catalysts for the visible-light driven SMRs at ambient conditions [26]. Among the various Pd-non-noble metal NPs reported, Pd-Ni NPs are economical and effective catalysts for diverse transformations [27–31]. To date, a variety of protocols for the fabrication of Pd-Ni NPs have been developed by many research groups including chemical reduction methods, γ-irradiation, electrodeposition, template-directed fabrication, etc [15,18,32–37]. Despite the progress in this field, there are still some problems frequently encountered with the reported Ni-Pd bimetallic nanocatalysts, such as low atom efficiency,

limited substrate scope, degradation, and the leaching of the metal species. In our continuous effort to develop efficient and stable bimetallic nanocatalysts for the SMRs, we reasoned that the loading of Pd-Ni bimetallic NPs onto TiO_2 nanopowders would not only retain their catalytic performance but also improve their stability. To the best of our knowledge, there have had no reports on the use of such materials for the SMRs.

In this paper, we successfully prepared TiO_2-supported Pd-Ni nanoparticles with the mean diameter of approximately two nanometers through a one-step impregnation-reduction route. The as-prepared Pd-Ni/TiO_2 exhibited enhanced catalytic activity compared to an equal amount of Pd/TiO_2 as well as excellent stability and recyclability in the SMRs.

2   Materials and methods

2.1   Chemicals

$PdCl_2$, $NiCl_2 \cdot 6H_2O$, NaOH, and $NaBH_4$ were of analytical reagent grade and supplied by Sinopharm Chemical Reagent Co., Ltd (Shanghai, China). The $PdCl_2$ solution was prepared by dissolving 1.0 g of $PdCl_2$ into 50 mL of HCl (1.0 mol/L) and was stored in the refrigerator at 4 °C prior to use. TiO_2 P25 was supplied from Degussa (Hulls Corporation, Germany). Iodobenzene and phenylboronic acid series were purchased from Aladdin Industrial Cooperation. All Chemicals were used without further purification.

2.2   Catalyst preparation

The catalyst was prepared by a one-step impregnation-reduction method. For example, to synthesize 1–n wt-% Pd-Ni/TiO_2 (n = 0.5, 1.0, 2.0, 3.0, 5.0), firstly 40.5n mg (0.1704n mmol) $NiCl_2 \cdot 6H_2O$ and 833 μL of the $PdCl_2$ solution were added into 50 mL of distilled water via stirring. P25 TiO_2 powder (1000 mg) was then dispersed into the mixed solution, and the slurry was placed in an oil bath with stirring to maintain a temperature of 80 °C. After impregnation of the two precursors on TiO_2 for 1 h, NaOH solution (1.0 mol/L) was added to tune the pH value to approximately 10. Then, 50 mL of aqueous $NaBH_4$ solution (1.0 g) was added dropwise to the suspension. After ageing for 10 h, the solid product was collected by vacuum filtration, and then washed thoroughly with distilled water, followed by vacuum drying at 60 °C overnight.

2.3   Characterization

The elemental analysis of the catalysts was performed by a Thermo Scientific iCAP 6300 Inductively Coupled Plasma Optical Emission Spectrometry (ICP-OES). The crystal structures of the samples were characterized by a PANalytical X'Pert PRO X-ray diffractometer (XRD) with Cu Kα radiation. Transmission electron microscopy (TEM) images were obtained using a JEM 2100 microscope while energy-dispersive spectrometry (EDS) was assessed using a JEM 2100F instrument, using a copper grid coated with an ultrathin carbon film as the substrate. X-ray photoelectron spectroscopy (XPS) results were obtained from a Thermo Scientific Escalab 250Xi X-ray photoelectron spectrometer using a monochromatic aluminum Kα X-ray source at 20 kV. The binding energies of all measurements were calibrated using the C 1s peak at 284.6 eV. High performance liquid chromatography (HPLC) results were obtained by a Waters 1525 machine with a Waters 2487 dual λ absorbance detector and a C18 column using methanol/H_2O = 4/1 as mobile phase at λ = 254 nm, 30 °C, and 1 mL/min (flow rate). ^{1}H NMR and ^{13}C NMR spectra were recorded on a Bruker 400 MHz NMR spectrometer in $CDCl_3$ (δ values are referred to $CHCl_3$ at 7.26 ppm and 77.0 ppm, respectively).

2.4   General procedure of Suzuki-Miyaura coupling reaction

In a typical reaction, the mixture of water (1.0 mL), ethanol (1.0 mL), K_2CO_3 (82.9 mg, 0.6 mmol), iodobenzene (0.2 mmol), benzeneboronic acid (0.3 mmol), and the Pd-Ni/TiO_2 catalyst (an equivalent amount to 0.002 mmol of Pd) was added to a flask placed in an oil bath with stirring to maintain a temperature of 50 °C for 5 h. After the reaction, the solid catalyst was separated via centrifugation and then washed thoroughly with distilled water and ethanol, followed by the removal of solvent under vacuum at 60 °C overnight. The collected sample was reused for the target reaction.

3   Results and discussion

3.1   Catalyst characterization

3.1.1   ICP-OES results

We prepared five Pd-Ni/TiO_2 catalysts (numbered I, II, III, IV and V) with different amount ratios of Ni and Pd precursors (0.5, 1.0, 2.0, 3.0, and 5.0). The results of elemental analysis by ICP-OES are shown in Table 1. The obtained ratios of Ni and Pd in catalyst I to V were 0.47, 0.97, 1.99, 2.95, and 5.20 respectively, which fit well with those in the added precursors.

3.1.2   X-ray diffraction (XRD) analysis

XRD patterns (Fig. 1) of the Pd-Ni/TiO_2 catalysts with different amount ratios of Ni and Pd as well as Pd/TiO_2, Ni/TiO_2 all show no differences with that of pure TiO_2 P25. All the strong diffraction peaks in their XRD patterns are

Table 1 ICP-OES data of the Pd-Ni/TiO$_2$ catalysts

Entry	Amount in the added precursors			ICP-OES data		
	Pd /wt-%	Ni /wt-%	Ni : Pd	Pd /wt-%	Ni /wt-%	Ni : Pd
I	1.0	0.5	0.5	0.99	0.47	0.47
II	1.0	1.0	1.0	0.94	0.91	0.97
III	1.0	2.0	2.0	0.96	1.92	1.99
IV	1.0	3.0	3.0	0.89	2.62	2.95
V	1.0	5.0	5.0	0.84	4.35	5.20
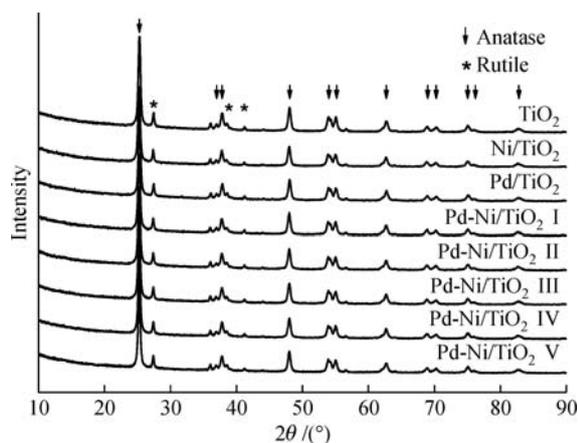
Fig. 1 XRD patterns of the Pd-Ni/TiO$_2$ catalysts, Pd/TiO$_2$, Ni/TiO$_2$, and TiO$_2$ P25

easily indexed to TiO$_2$ P25, which consists of anatase (JCPD-78-2486) and rutile (JCPD-76-1938), implying that the supported Pd-Ni NPs have no influence on the crystal structure of the TiO$_2$ supports. The reason why there is no new peak, which could be indexed to Pd or Ni, is

presumably that the proportion of the loaded metals is too low to be detected.

3.1.3 Transmission electron microscopy (TEM) analysis

TEM analysis of the Pd-Ni/TiO$_2$ IV catalyst (Fig. 2) reveals the morphology and particle size of the Pd-Ni nanocrystals. The spherical Pd-Ni alloy NPs (NPs) disperse uniformly on the TiO$_2$ surface with the mean diameter of approximately two nanometers (Fig. 2(b)). The high-resolution TEM (HR-TEM) image (Fig. 2(c)) shows lattice diffraction fringes with interplanar spacing of 0.126 nm on the NPs, which match well with that of the (220) plane of the face-centered cubic (FCC) Pd-Ni alloy. The EDS mapping of Ni and Pd in a single metal NP (Figs. 2(d–f)) show that the NPs consist of both Pd and Ni, indicating that the two metals exist as a binary alloy in this material.

3.1.4 XPS analysis

XPS was used to analyze the oxidation states of Pd and Ni in the Pd-Ni/TiO$_2$ (Fig. 3). The Pd 3d and Ni 2p spectra all
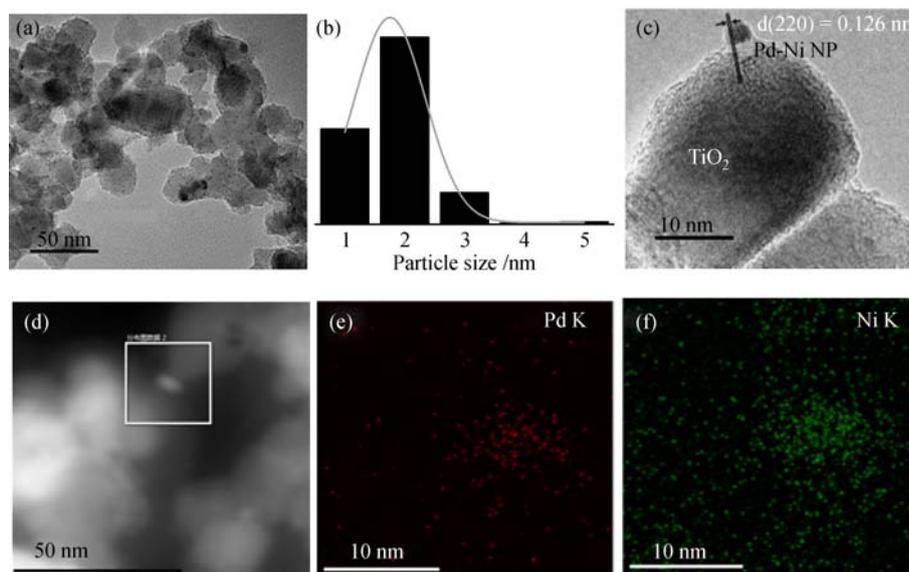
Fig. 2 (a) TEM image, (b) particle size distribution, (c) HR-TEM image of the Pd-Ni NPs, (d) HAADF-STEM image of one single Pd-Ni NP, and EDS mapping of (e) Pd and (f) Ni of the Pd-Ni/TiO$_2$ IV catalyst
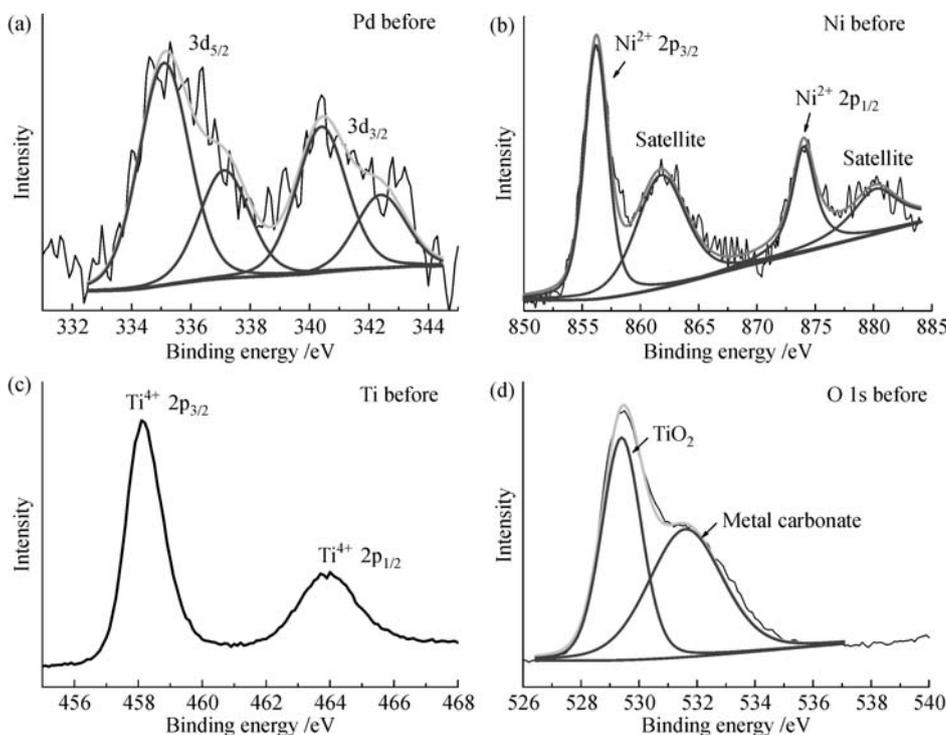
Fig. 3 XPS results of (a) Pd 3d, (b) Ni 2p, (c) Ti 2p, and (d) O1s of the Pd-Ni/TiO$_2$ IV catalyst

exhibit two contributions resulting from spin-orbit splitting. The main peaks of Pd 3d$_{5/2}$ and 3d$_{3/2}$ are located at 335.1 and 340.4 eV, respectively, which are assigned to the Pd(0) species. In addition, the existence of Pd(II) is evidenced by shoulders observed on the right of the main peaks located at 337.1 and 342.3 eV after the peak fitting, respectively. The percentage of Pd(II) is estimated to be 31% in the Pd-Ni/TiO$_2$ catalyst. Besides, the main peaks of Ni 2p$_{3/2}$ and 2p$_{1/2}$ that located at 856.2 and 874.0 eV respectively are assigned to the Ni(II) species, indicating that there is no Ni in zero valence state in the Pd-Ni/TiO$_2$ catalyst. The two other peaks in the Ni 2p spectra are assigned to the satellites of Ni(II) species. Moreover, the

XPS spectrum of Ti 2p exhibits two main peaks which are assigned to Ti(IV) species. Finally, the peak in the O 1s spectra is broad with two overlapping components. After peak differentiating and imitating, apart from the peak assigned to TiO$_2$ (located at 529.5 eV), the other was assigned to carbonates from water and organic contamination in the process of preparation and storage.

3.2   Catalytic activity

To test the catalytic activities of the Pd-Ni/TiO$_2$ catalysts for the SMRs, the coupling reaction of iodobenzene and 4-methylphenylboronic acid is selected as a model reaction

Table 2   Catalyst survey for the Suzuki–Miyaura coupling reaction of iodobenzene and 4-methylbenzeneboronic acid [a]
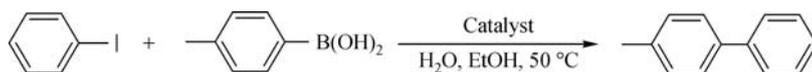
Entry	Catalyst	Yield /% [b]
1	TiO$_2$	–
2	Ni/TiO$_2$	trace
3	Pd/TiO$_2$	86.2
4	Pd-Ni/TiO$_2$ I	91.3
5	Pd-Ni/TiO$_2$ II	92.9
6	Pd-Ni/TiO$_2$ III	94.3
7	Pd-Ni/TiO$_2$ IV	97.2
8	Pd-Ni/TiO$_2$ V	93.8

a) Reaction conditions: 1.0 mL of water, 1.0 mL of ethanol, 0.6 mmol of K$_2$CO$_3$, 0.2 mmol of iodobenzene, 0.3 mmol of 4-methylbenzeneboronic acid and an amount of catalyst equivalent to 0.002 mmol Pd, 50 °C, 5 h; b) yields were determined by HPLC with 4-methylbiphenyl as the external standard

(Table 2). The reaction did not occur with pure TiO_2 P25 as the catalyst. All the bimetallic Pd-Ni/TiO_2 catalysts exhibited excellent catalytic activity under the given conditions (entries 4–8). For the control experiments with Ni/TiO_2 and Pd/TiO_2, trace amount and 86.2% yield of the corresponding product were obtained, respectively (entries 2–3). Among the five Pd-Ni/TiO_2 catalysts evaluated, IV showed the best activity, furnishing the product in 97.2% yield.

3.3 Stability and recyclability

To investigate the stability and reusability of the Pd-Ni/TiO_2 catalyst, Pd-Ni/TiO_2 IV was recycled four times by centrifugation in the Suzuki–Miyaura coupling reaction of iodobenzene with 4-methylbenzeneboronic acid (Fig. 4). There was almost no loss in catalytic activity, indicating the admirable recyclability of the Pd-Ni/TiO_2 catalyst.
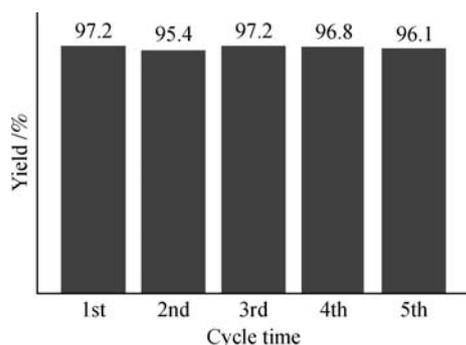
Fig. 4 Recyclability of the Pd-Ni/TiO_2 IV catalyst in the Suzuki-Miyaura coupling reaction of iodobenzene with 4-methylbenzeneboronic acid. Yields were determined by HPLC on the basis of 4-methylbiphenyl

Figure 5 shows the TEM analysis of the Pd-Ni/TiO_2 IV catalyst after four cycles. The Pd-Ni NPs are still spherical and dispersed uniformly on the TiO_2 surface with a mean diameter of about two nanometers (Fig. 5(b)). The HR-TEM image (Fig. 5(c)) show that the NPs of the recycled catalyst present the same FCC Pd-Ni alloy lattice with a (220) interlayer spacing of 0.127 nm. In the EDS mapping of Ni and Pd in a single metal NP of the recycled catalyst (Figs. 5(d–f)), Pd and Ni still exist as a binary alloy after recycling. Hence, there is obviously neither aggregation nor change in both morphology and composition of the Pd-Ni NPs, implying the benign stability of the Pd-Ni/TiO_2 catalyst.

Figure 6 shows the XPS results of the Pd-Ni/TiO_2 IV catalyst after four cycles. The main peaks of Pd are located at 334.3 and 339.2 eV, which are assigned to the Pd(0) species, with two shoulders located at 336.3 and 341.5 eV, which are assigned to the Pd(II) species. The estimated percentage of Pd(II) increased to 49% in the recycled Pd-Ni/TiO_2 IV catalyst, whereas the main peaks in the Ni 2p, Ti 2p and the O 1s spectra have no change. The XPS results demonstrated that there is only little rise in the oxidation states of Pd in the Pd-Ni/TiO_2 IV catalyst after four cycles, indicating the commendable stability of the catalyst.

3.4 General applicability

After the reaction conditions were optimized, we further tested the feasibility of the Pd-Ni/TiO_2 IV as a catalyst for a series of Suzuki Miyaura coupling reactions between substituted aryl halides and aryl boronic acids (Table 3). All the phenylboronic acids and iodobenzenes bearing with either an electron-donating group or an electron-withdrawing group (entries 1–4) show excellent reactivity, giving the corresponding product in excellent yields,
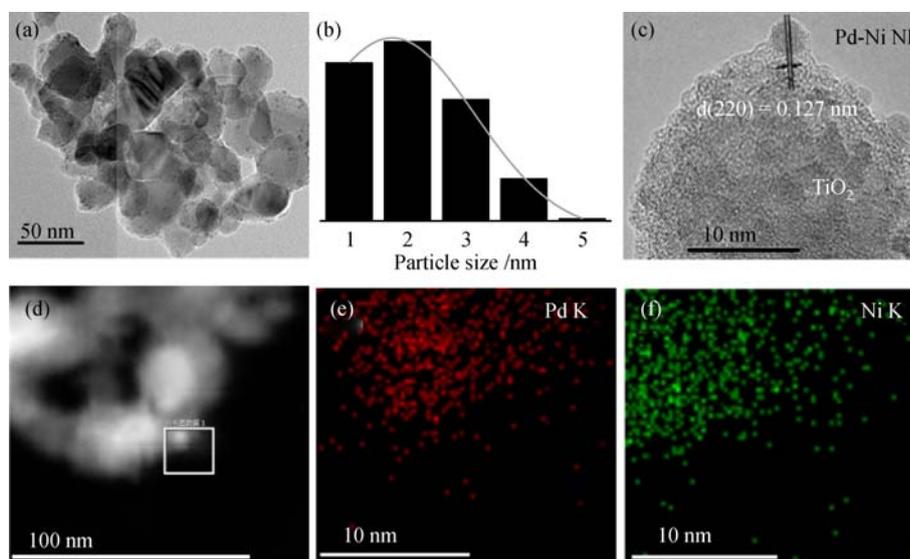
Fig. 5 (a) TEM image, (b) particle size distribution, (c) HR-TEM image of the Pd-Ni NPs, (d) HAADF-STEM image of one single Pd-Ni NP, and EDS mapping of (e) Pd and (f) Ni of the Pd-Ni/TiO_2 IV catalyst after four cycles
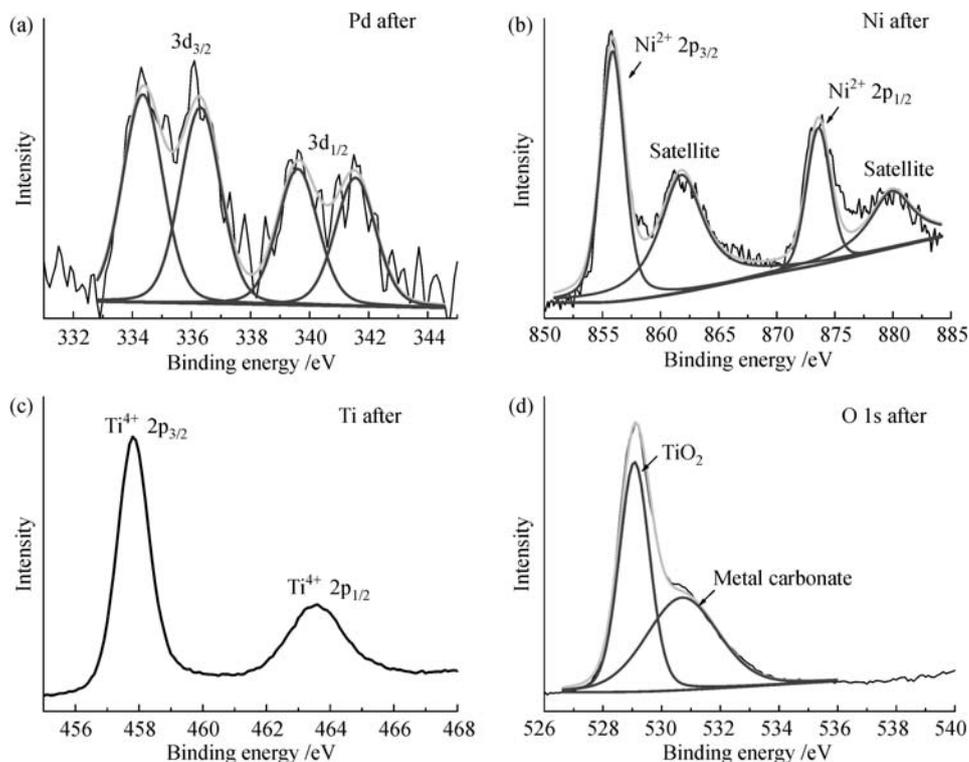
Fig. 6   XPS results of (a) Pd 3d, (b) Ni 2p of the Pd-Ni/TiO$_2$ IV catalyst after four cycles, (c) and (d)

Table 3   Substrate scope of the Suzuki–Miyaura coupling reaction catalyzed by Pd-Ni/TiO$_2$ IV[a)]
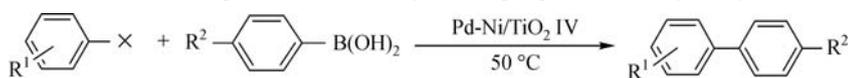
Entry	X	R^1	R^2	Yield /%[b)]
1	I	H	OCH$_3$	99
2	I	H	COCH$_3$	99
3	I	p-COCH$_3$	H	99
4	I	p-OCH$_3$	H	99
5	I	m-OCH$_3$	H	96
6	I	o-OCH$_3$	H	89
7	Br	H	CH$_3$	91
8	Cl	H	CH$_3$	11
9	I	p-Cl	H	98

a) Reaction conditions: water (1 mL), ethanol (1 mL), K$_2$CO$_3$ (0.6 mmol), benzene halides (0.2 mmol), benzeneboronic acid (0.3 mmol), and an amount of catalyst equivalent to 0.002 mmol Pd, 50 °C, 5 h; b) isolated yields after chromatography

suggesting that both electron-donating and electron-with-drawing groups have neglectable effect on the reactivity. It is noteworthy that iodobenzenes with a methoxy group at *meta*- and *ortho*- position gave the corresponding products in slightly lower yields of 96% and 89% respectively (entries 5–6), presumably owing to the change of electronic or steric properties. Bromobenzene and chlorobenzene afforded the biphenyl products in 91% and 11% yields (entries 7–8), respectively, which could be attributed to the different electronegativity of halogen elements (Cl

3.16, Br 2.96, I 2.66) [16,33]. Encouraged by these results, we further investigated the coupling reaction of phenyl-boronic acid with 1-chloro-4-iodobenzene (entry 9), and found that only iodine was replaced, indicating an excellent functional group selectivity.

4   Conclusions

In summary, we have successfully developed a Pd-Ni/TiO$_2$

catalyst for the SMRs through a one-step impregnation-reduction method. TEM analysis showed that the spherical NPs dispersed uniformly on the TiO_2 surface with a mean diameter of about two nanometers, which consisted of both Pd and Ni. The catalytic results show that the introduction of Ni to Pd improves the catalytic activities and the iodobenzenes and phenylboronic acids bearing with an electron-donating or electron-withdrawing group gave the corresponding product in excellent yields. Moreover, the Pd-Ni/TiO_2 catalyst exhibited excellent stability and recyclability that no considerable loss in catalytic activities was observed after four cycles.

References

1. Crane E A, Scheidt K A. Prins-type macrocyclizations as an efficient ring-closing strategy in natural product synthesis. Angewandte Chemie International Edition, 2010, 49(45): 8316–8326

2. Dumas A, Spicer C D, Gao Z, Takehana T, Lin Y A, Yasukohchi T, Davis B G. Self-liganded Suzuki-Miyaura coupling for site-selective protein PEGylation. Angewandte Chemie International Edition, 2013, 52(14): 3916–3921

3. Maluenda I, Navarro O. Recent developments in the Suzuki-Miyaura reaction: 2010–2014. Molecules (Basel, Switzerland), 2015, 20(5): 7528–7557

4. Miyaura N, Suzuki A. Stereoselective synthesis of arylated (E)-alkenes by the reaction of alk-1-enylboranes with aryl halides in the presence of palladium catalyst. Chemical Communications, 1979, 19(19): 866–867

5. Rossi R, Bellina F, Lessi M, Manzini C, Marianetti G A, Perego L. Recent applications of phosphane-based palladium catalysts in Suzuki-Miyaura reactions involved in total syntheses of natural products. Current Organic Chemistry, 2015, 19(14): 1302–1409

6. Yamaguchi J, Yamaguchi A D, Itami K. C–H bond functionalization: Emerging synthetic tools for natural products and pharmaceuticals. Angewandte Chemie International Edition, 2012, 51(36): 8960–9009

7. Yokoyama A, Suzuki H, Kubota Y, Ohuchi K, Higashimura H, Yokozawa T. Chain-growth polymerization for the synthesis of polyfluorene via Suzuki-Miyaura coupling reaction from an externally added initiator unit. Journal of the American Chemical Society, 2007, 129(23): 7236–7237

8. Pagliaro M, Pandarus V, Ciriminna R, Béland F, Demma Carà P. Heterogeneous *versus* homogeneous palladium catalysts for cross-coupling reactions. ChemCatChem, 2012, 4(4): 432–445

9. Que Y, Feng C, Zhang S, Huang X. Stability and catalytic activity of PEG-b-PS-capped gold nanoparticles: A matter of PS chain length. Journal of Physical Chemistry C, 2015, 119(4): 1960–1970

10. Chen J, Zhang Z, Bao Z, Su Y, Xing H, Yang Q, Ren Q. Functionalized metal-organic framework as a biomimetic heterogeneous catalyst for transfer hydrogenation of imines. ACS Applied Materials & Interfaces, 2017, 9(11): 9772–9777

11. Chtchigrovsky M, Lin Y, Ouchaou K, Chaumontet M, Robitzer M, Quignard F, Taran F. Dramatic effect of the gelling cation on the catalytic performances of alginate-supported palladium nanoparticles for the Suzuki-Miyaura reaction. Chemistry of Materials, 2012, 24(8): 1505–1510

12. Jiang B, Song S, Wang J, Xie Y, Chu W, Li H, Xu H, Tian C, Fu H. Nitrogen-doped graphene supported Pd@PdO core-shell clusters for C–C coupling reactions. Nano Research, 2014, 7(9): 1280–1290

13. Sun J, Fu Y, He G, Sun X, Wang X. Green Suzuki-Miyaura coupling reaction catalyzed by palladium nanoparticles supported on graphitic carbon nitride. Applied Catalysis B: Environmental, 2015, 165: 661–667

14. Zhang L, Feng C, Gao S, Wang Z, Wang C. Palladium nanoparticle supported on metal-organic framework derived *N*-decorated nanoporous carbon as an efficient catalyst for the Suzuki coupling reaction. Catalysis Communications, 2015, 61: 21–25

15. Ohtaka A, Sansano J M, Nájera C, Miguel-García I, Berenguer-Murcia Á, Cazorla-Amorós D. Palladium and bimetallic palladium-nickel nanoparticles supported on multiwalled carbon nanotubes: Application to carbon-carbon bond-forming reactions in water. ChemCatChem, 2015, 7(12): 1841–1847

16. Song H, Zhu Q, Zheng X, Chen X. One-step synthesis of three-dimensional graphene/multiwalled carbon nanotubes/Pd composite hydrogels: An efficient recyclable catalyst for Suzuki coupling reactions. Journal of Materials Chemistry. A, Materials for Energy and Sustainability, 2015, 3(19): 10368–10377

17. Hu J, Yang Q, Yang L, Zhang Z, Su B, Bao Z, Ren Q, Xing H, Dai S. Confining noble metal (Pd, Au, Pt) nanoparticles in surfactant ionic liquids: Active non-mercury catalysts for hydrochlorination of acetylene. ACS Catalysis, 2015, 5(11): 6724–6731

18. Wu Y, Wang D, Zhao P, Niu Z, Peng Q, Li Y. Monodispersed Pd-Ni nanoparticles: Composition control synthesis and catalytic properties in the Miyaura-Suzuki reaction. Inorganic Chemistry, 2011, 50(6): 2046–2048

19. Cai S, Wang D, Niu Z, Li Y. Progress in organic reactions catalyzed by bimetallic nanomaterials. Chinese Journal of Catalysis, 2013, 34(11): 1964–1974

20. Gu J, Zhang Y W, Tao F. Shape control of bimetallic nanocatalysts through well-designed colloidal chemistry approaches. Chemical Society Reviews, 2012, 41(24): 8050–8065

21. Chen T, Rodionov V O. Controllable catalysis with nanoparticles: Bimetallic alloy systems and surface adsorbates. ACS Catalysis, 2016, 6(6): 4025–4033

22. Shaabani A, Mahyari M. PdCo bimetallic nanoparticles supported on PPI-grafted graphene as an efficient catalyst for Sonogashira reactions. Journal of Materials Chemistry. A, Materials for Energy and Sustainability, 2013, 1(32): 9303–9311

23. Nath Dhital R, Kamonsatikul C, Somsook E, Sakurai H. Bimetallic gold-palladium alloy nanoclusters: An effective catalyst for Ullmann coupling of chloropyridines under ambient conditions. Catalysis Science & Technology, 2013, 3(11): 3030–3035

24. Tan L, Wu X, Chen D, Liu H, Meng X, Tang F. Confining alloy or

core-shell Au-Pd bimetallic nanocrystals *in silica* nanorattles for enhanced catalytic performance. Journal of Materials Chemistry. A, Materials for Energy and Sustainability, 2013, 1(35): 10382–10388

25. Alonso A, Shafir A, Macanás J, Vallribera A, Muñoz M, Muraviev D N. Recyclable polymer-stabilized nanocatalysts with enhanced accessibility for reactants. Catalysis Today, 2012, 193(1): 200–206

26. Han D, Bao Z, Xing H, Yang Y, Ren Q, Zhang Z. Fabrication of plasmonic Au-Pd alloy nanoparticles for photocatalytic Suzuki-Miyaura reactions under ambient conditions. Nanoscale, 2017, 9 (18): 6026–6032

27. Wilson D A, Wilson C J, Rosen B M, Percec V. Two-step, one-pot Ni-catalyzed neopentylglycolborylation and complementary Pd/Ni-catalyzed cross-coupling with aryl halides, mesylates, and tosylates. Organic Letters, 2008, 10(21): 4879–4882

28. Son S U, Jang Y, Park J, Na H B, Park H M, Yun H J, Lee J, Hyeon T. Designed synthesis of atom-economical Pd/Ni bimetallic nanoparticle-based catalysts for Sonogashira coupling reactions. Journal of the American Chemical Society, 2004, 126(16): 5026–5027

29. Heshmatpour F, Abazari R, Balalaie S. Preparation of monometallic (Pd, Ag) and bimetallic (Pd/Ag, Pd/Ni, Pd/Cu) nanoparticles via reversed micelles and their use in the Heck reaction. Tetrahedron, 2012, 68(14): 3001–3011

30. Takenaka S, Shigeta Y, Tanabe E, Otsuka K. Methane decomposition into hydrogen and carbon Nanofibers over supported Pd-Ni catalysts: Characterization of the catalysts during the reaction. Journal of Physical Chemistry B, 2004, 108(23): 7656–7664

31. Feng L, Chong H, Li P, Xiang J, Fu F, Yang S, Yu H, Sheng H, Zhu M. Pd-Ni alloy nanoparticles as effective catalysts for Miyaura-Heck coupling reactions. Journal of Physical Chemistry C, 2015, 119(21): 11511–11515

32. Xiang J, Li P, Chong H, Feng L, Fu F, Wang Z, Zhang S, Zhu M. Bimetallic Pd-Ni core-shell nanoparticles as effective catalysts for the Suzuki reaction. Nano Research, 2014, 7(9): 1337–1343

33. Xia J, Fu Y, He G, Sun X, Wang X. Core-shell-like Ni-Pd nanoparticles supported on carbon black as a magnetically separable catalyst for green Suzuki-Miyaura coupling reactions. Applied Catalysis B: Environmental, 2017, 200: 39–46

34. Metin Ö, Ho S F, Alp C, Can H, Mankin M N, Gültekin M S, Chi M, Sun S. Ni/Pd core/shell nanoparticles supported on graphene as a highly active and reusable catalyst for Suzuki-Miyaura cross-coupling reaction. Nano Research, 2013, 6(1): 10–18

35. Kim M R, Choi S H. One-step synthesis of Pd-M/ZnO (M = Ag, Cu, and Ni) catalysts by irradiation and their use in hydrogenation and Suzuki reaction. Journal of Nanomaterials, 2009, 2009: e302919

36. Kim S J, Oh S D, Lee S, Choi S H. Radiolytic synthesis of Pd-M (M = Ag, Ni, and Cu)/C catalyst and their use in Suzuki-type and Heck-type reaction. Journal of Industrial and Engineering Chemistry, 2008, 14(4): 449–456

37. Han F S. Transition-metal-catalyzed Suzuki-Miyaura cross-coupling reactions: A remarkable advance from palladium to nickel catalysts. Chemical Society Reviews, 2013, 42(12): 5270–5298